

## Localization Effects in Torsion Shear Tests on Sand

Jung-Man Nam

*Dept. of Ocean Civil Engrg. Cheju National University Cheju-do 690-756, Korea*

### 모래에 대한 비틀림전단시험에서 변형률 국부효과

남정만

제주대학교 해양토목공학과

Santa Monica 해변 모래에 대한 비틀림 전단시험을 실시한 결과 증공원통형 공시체에서 변형률 국부현상이 관찰되었다. 변형률 국부현상은 평면변형 상태에서부터 시작되었으며 삼축인장시험시에는 아주 중요한 문제를 야기시킬 수 있다. 변형률 국부현상은 shear band나 necking의 현상으로부터 파괴가 발생하기 전에 발생하므로 응력비가 평면변형상태 이후에서는 파괴강도가 낮게 측정되어 진다. 비틀림전단시험기에서 경계조건의 기하학적 특성은 membrane에 어떠한 구속을 가하지 않은 상태에서도 변형률국부현상이 쉽게 발생하였다. 그리고 이러한 영향은 균등한 변형이 발생하는 삼차원 파괴기준과는 다른 결과를 나타나게 한다.

Serious strain localization could be observed in hollow cylinder specimens in torsion shear tests on Santa Monica Beach Sand. The strain localization began at plane strain and was most significant at triaxial extension. Since the strain localization produced premature development of shear bands or necking, lower strength was measured at and beyond plane strain. The geometric configuration of the boundaries in torsion shear apparatus is easy to produce shear bands due to strain localization, which is developed freely without significant restraint from the soft side rubber membranes. The strain localization affects the measurement of strength, and these effects lead to different three dimensional failure criteria. One is excessively affected by strain localization and the other corresponds to uniform strains.

**Key words** : torsion shear test, strain localization, shear band, necking, failure criteria, plane strain, triaxial test, friction angle

### INTRODUCTION

Experimental studies on soil elements have presented many significant information for modeling soil behavior. Right information thus have been always required for any stress condition to cover the full range of stresses from triaxial compression to

triaxial extension. Sometimes however it was hard to get true data because of some limitations of experimental devices. In 1963, Roscoe et al. encountered many problems associated with strain localization, especially, in triaxial extension test. Therefore they concluded that it was impossible to evaluate the failure criteria until a testing method

to get uniform strains was developed.

During last few decades, there was outstanding development of experimental devices and techniques to ensure uniformity of strain in soil specimens. Lade(1982) presented some techniques to eliminate the effect of the end restraint and the nonuniformity of strains on soil behavior. And many cubical triaxial devices were built to observe three dimensional behavior under uniform strain (Arthur(1988)). However, the cubical triaxial device does not allow for a continuous rotation of principal stresses. To improve this limitation, torsion shear and simple shear devices were developed (Saada(1988)). Talesnick and Frydman(1991) indicated that the torsion shear device is most suitable tool at the present time, whereas the simple shear device can not ensure uniformity of strain in the specimen.

In order to obtain reliable data from the torsion shear device, the specimen should be tall enough to make uniform strain in central zone, so that effects of end restraint could be neglected(Lade(1981)). And the inner and the outer cell pressures should be same to ensure uniform distribution of radial horizontal strain in hollow cylinder specimen (Lade(1981)), Saada(1988)).

Many investigators have observed that extension tests on cylindrical specimens produced results that are heavily affected by premature by premature development of shear plane due to strain localization(Roscoe et al.(1963),Lade(1982b), Peter et al.(1988), Yamamuro and Lade(1995)). Strain localization also was observed in other tests such as triaxial compression tests, plane strain tests, simple shear tests and torsional simple shear tests (Arthur et al.(1975), Tatsuoka et al.(1970), Lade et al.(1994)). The stress-strain behavior, the volume change and the strength are heavily affected by the strain localization.

The purpose of the present study is to observe

where the effects of strain localization invalidate strength measurement in torsion shear tests. A series of torsion shear tests was performed along various stress-paths on hollow cylinder specimens of Santa Monica Beach Sand. The stress paths were decided to cover the full range of vertical deviator stresses from compression to extension. For comparison with the torsion shear tests, a series of cubical triaxial tests were performed on the same sand along various stress paths from triaxial compression to triaxial extension. The strengths obtained from both tests were compared and reviewed.

## PREVIEW STUDIES OF STRAIN LOCALIZATION

End restraint in hollow cylinder specimen affects the uniformity of strain distributions during testing. Lade(1981) showed experimentally that the tangential horizontal stress in hollow cylinder specimen had much the influence of the end restraint, and to minimize nonuniformities of stress and strain, the ratio of height to average diameter of specimen should be equal to or higher than one. Saada(1988) showed similar results by summarizing the specimen dimensions and bounding effects for the hollow cylinder specimens used in torsion shear devices by many investigators.

Strain localization is induced by the nonuniformity of strain distribution and produce premature shear plane. The strain localization can have a very significant effect pm strength, stress-strain behavior, volume change characteristics of sand(Fukushima and Tatsuoka 1982). Lade(1982) indicated that line failure involves only a small part of the specimen and generally the loosest part, whereas zone failure involves the entire specimen and provide a better measure of the soil properties at the average specimen density.

Many investigators have observed shear band or

## LOCALIZATION EFFECTS IN TORSION SHEAR TESTS ON SAND

necking in specimens due to strain localization in various experimental devices (Arthur et al. 1977; Peter et al. 1988; Tatsuoka et al. 1990; Scarpelli and Wood 1992; Lade et al. 1944). The shear bands are initiated more easily under triaxial extension tests than triaxial compression tests (Roscoe et al. 1963. Yamamuro and Lade 1995) developed a method to enforce uniform strains in triaxial extension tests on cylindrical specimens by the use of small metal plates separated by lubricated latex membranes. Peter et al. (1988) showed experimentally and theoretically that shear bands are initiated more easily under plane strain than under axially symmetric conditions of the triaxial test. Atkinson and Richardson (1987) observed that local drainage occurred in shear zone on undrained test of overconsolidated clay and produced the consequent reduction in apparent undrained strength.

The shear bands are oriented at specific angle determined by the internal friction angle, the angle of dilation, and the particle size (Arthur et al. 1977; Arthur and Dunstan 1982). Tatsuoka et al. (1990) investigated the shear band direction related to the directions of the bedding plane the Coulomb plane, and the Roscoe plane. Cole and Lade (1984) showed that the direction of rupture plane in alluvium over active dip slip faults is controlled by the angle of dilation of the soil.

## EXPERIMENTAL EQUIPMENT

### Torsion Shear Apparatus

A torsion shear apparatus was designed was designed and built permit individual control of confining pressure, vertical deviator stress and shear stress to a hollow cylinder specimen. The entire setup is contained in a pressure cell. The details of the torsion shear apparatus were described elsewhere

(Hong and Lade 1989a, 1986b). The same confining pressure was applied to the inside and the outside surfaces of specimens. The confining pressure is provided by the chamber pressure. The vertical load and the torque can be applied independently to the specimen through the center shaft and the cap plate, which is attached to the cap ring. Both the vertical load and the torque can be either stress- or strain-controlled. The hollow cylinder specimen was contained between the cap and base rings and the inside and outside surrounding membranes. The specimen employed for testing on sand has an average diameter of 20 cm, a wall thickness of 2 cm, and heights of 25 cm and 40 cm. The average values of horizontal deformations and changes in thickness of specimen wall are calculated from the relationship between the measurements of the volume changes in the inside chamber and specimen and the vertical deformations. The detail derivation of equations to calculate the horizontal strains was given in a companion study (Hong, Nam and Lade 1995).

### Cubical Triaxial Apparatus

A cubical triaxial apparatus was designed to permit application of three unequal principal stresses to a cubical specimen with side lengths of 76 mm. The details of this apparatus were described elsewhere (Lade and Duncan 1973; Lade and Musante 1978). The specimen was contained between a cap and base a surrounding membrane. The minor principal stress was provided by the chamber pressure. The vertical deviator stress provided by the vertical load and the chamber pressure. The horizontal deviator stress was applied by the chamber pressure and a horizontal loading system. Both the horizontal loading plates and the cap and base were provided with lubricated surfaces. The boundary condition of this apparatus is enforced

uniform strain distribution by the loading devices. Shear planes can be suppressed in specimen during cubical triaxial tests, since uniform strain is developed in the specimen.

## SPECIMEN PREPARATION

### Sand Tested

All tests were performed on sand obtained from in Santa Monica, California. The sand was washed several times with fresh water to eliminate salt and impurities, and the portion passing the No.40 sieve (sieve opening = 0.425mm) was used for testing. The specific gravity was 2.66. The coefficient of uniformity was 1.58 and the particle shapes show angular to subangular. Mineral composition is 45% feldspar, 8% magnetite and 2% trace minerals. The maximum and minimum void ratios were, respectively, 0.91 and 0.60.

### Hollow Cylinder Specimens

The hollow cylinder specimens were prepared by the air pluviation through a tube with a diameter of 1m. The tip of the tube kept always 15cm above the deposition level.

The falling velocity of sand was adjusted by a mesh with 2.5mm opening, attached on the tip of the tube. The preweighted amount of dry sand was pluviated into the specimen cavity formed by the base ring and the inside and outside membranes held by the forming jackets. The predetermined height, 25cm and 40cm, of specimens were obtained by tapping slightly the cap ring and the outside forming jacket with soft hammer. After setting the membrane to the cap ring, a small vacuum of  $0.5\text{kg}/\text{cm}^2$  (49kPa) was applied and the specimen dimensions were measured. A grid consisting of approximately spaced vertical and horizontal lines

was drawn on the surface of the outside membrane. After applying a initial confining pressure of  $0.5\text{kg}/\text{cm}^2$  (49kPa), the vacuum was eliminated and the dry specimen was saturated using the carbon dioxide method combined with back pressure to ensure a high degree of saturation (Lade and Duncan 1973). During test, a cell pressure of  $4.00\text{kg}/\text{cm}^2$  (392kPa) and a back pressure of  $2.00\text{kg}/\text{cm}^2$  (196kPa) were applied. The B-values measured before torsion tests indicated that the specimens were fully saturated.

The hollow cylinder specimens had an average relative density of 70% and averaged 22cm in outside diameter, 1cm in thickness, and 40cm and 25cm in heights of tall and short specimens, respectively.

### Cubical Specimens

The cap and base were coated with thin layers of silicon grease and covered with rubber sheets. The specimens were prepared directly on the base. A rubber membrane was stretched around the base and sealed with two O-rings, the rails which carry the horizontal loading system were fastened in place and the vacuum forming jacket was centered over the base and supported by the rails. The membrane was then stretched up through and around the forming jacket and a vacuum was applied. A measured quantity of dry sand was poured in the membrane and deposited to a small overheight, and the forming jacket was tapped with a soft hammer until the desired height and consequent density was achieved. The cap was then centered on the specimen and the rubber membranes stretched up and around the cap. The membrane was sealed to the cap with two O-rings. The top drainage line was connected to the cap and a vacuum applied to the specimen through a bubble chamber in order to detect leaks. If leak was detected, the specimen was painted with layers of rubber latex until the leak

was repaired. The dry specimen was saturated using the carbon dioxide method same as the hollow cylinder specimen.

The B-value measured before tests indicated that the specimens were fully saturated. The cubical specimens had an average relative density of 70% and average  $49 \text{ cm}^2$  in area and 7cm in height.

### TESTING PROGRAM

#### Torsion Shear Tests

Thirty four drained torsion shear tests were performed on hollow cylinder specimens of sand. Twenty six tests were performed on the tall specimens with height of 40cm. Fourteen tests out of the twenty six tests were performed to investigate the effect of stress rotation on the soil behavior during primary loading of small stress reversal, whereas eight tests were performed to investigate the soil behavior during large stress reversal. Eight tests on the short specimens with height of 25 cm were performed to investigate the effect of the specimen-height on the soil behavior in hollow cylinder specimens.

Each test was conducted with constant confining pressure  $\sigma_r$ , according to predetermined stress-paths shown in Fig. 1. The diagrams in this figures indicate relations between the vertical stress difference,  $(\sigma_z - \sigma_\theta)$ , and the torsion shear,  $\tau_{z\theta}$ . In order to follow these stress paths to failure and beyond, either the vertical stress difference or the torsion shear stress was applied under strain-control, and the stress was stress-controlled. The vertical stress difference could be either increased or decreased and the torque could be supplied in either a clockwise or a counterclockwise direction. Strain rate of 0.005%/min was employed for both vertical strain in the strain-controlled directions.

After setting the specimens, appropriate combina-

tions of the vertical load and the torque were applied to the hollow cylinder specimens, such that the major principal stress rotated from initial direction. A triaxial compression test and a triaxial extension test were performed on the tall specimens by, respectively, increasing and decreasing the vertical load under strain control as shown in Fig. 1(b). Torsional simple shear tests were performed on both tall and short specimens by the increasing the torque under strain control as shown in Fig. 1(b) and (c). Other tests were performed along the stress-paths shown in Fig. 1(b) and (c) by controlling the vertical load and the torque.

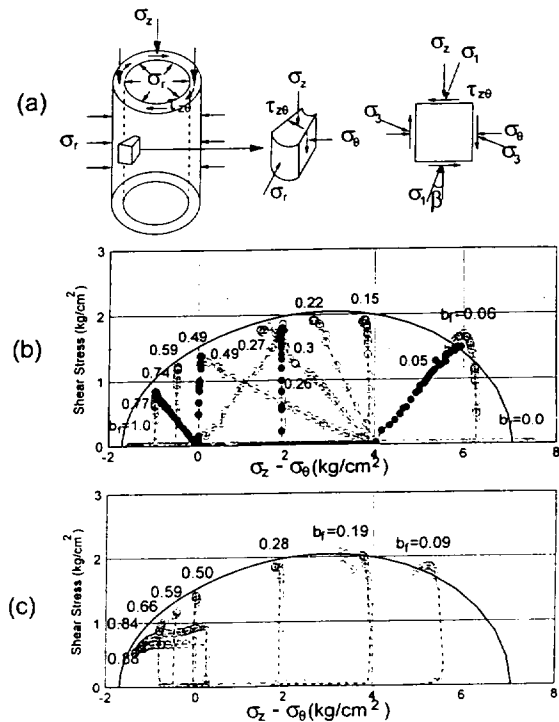


Fig. 1. (a) Stress in hollow cylinder specimen. (b) Stress-paths in torsion shear tests on tall specimens (height of 40cm). (c) Stress-paths in torsion shear tests on short specimens (height of 25cm).

#### Cubical Triaxial Tests

For comparison with the torsion shear tests, twelve drained tests were performed in cubical triaxial apparatus at four kinds of chamber pressures of  $0.5\text{kg/cm}^2(49\text{kPa})$ ,  $0.6\text{kg/cm}^2(59\text{kPa})$ ,  $1.0\text{kg/cm}^2(98\text{kPa})$  and  $2.0\text{kg/cm}^2(196\text{kPa})$ . Each test was conducted with constant confining pressures during tests according to the stress paths shown in Fig. 2. The diagrams in this figures represent the relations between the vertical and horizontal deviator stress, which are normalized by confining pressures. The stress paths are represented by the ratio between the deviator stresses denoted by  $b[(\sigma_2 - \sigma_3)/(\sigma_1 - \sigma_3)]$ . Each test was conducted with constant value of  $b$  throughout. In order to follow these stress paths to failure and beyond, the horizontal and the vertical deviator stresses were increased proportionally. The values of  $b$  used in the tests were chosen so that the failure surfaces and stress-strain behavior could be determined over the full range of the intermediate principal stress.

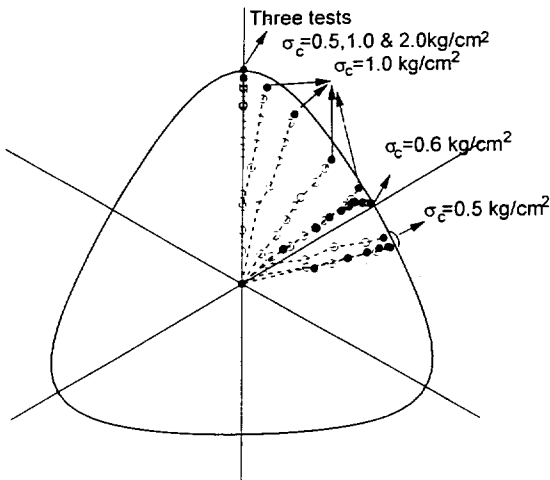


Fig. 2. Stress-paths for cubical triaxial tests on Santa Monica Beach Sand.

The vertical deviator stress was provided by strain control, in which strain rate of  $0.05\%/min$

was employed, whereas the horizontal deviator stress was provided by stress-control.

### OBSERVED STRENGTH CHARACTERISTICS

In order to investigate the strength characteristics observed in the torsion shear tests, the strength results have been compared internally and with also compared with those predicted by an isotropic three-dimensional failure criterion for soils. For torsion shear tests with the same inside and outside pressures, the effects of  $b (= \sin^2\Psi)$  and of the orientation of major principal stress (as measured by  $\Psi$ ) can not be separately examined, whereas the cubical triaxial tests are used to investigate only the effect of  $b$ . However, since the sand was essentially isotropic in behavior, the effect of  $b$  is described by the isotropic three-dimensional failure criterion.

#### Failure Criterion

A three-dimensional failure criterion expressed in terms of stress invariants has previously been developed for frictional material, such as clay, concrete and rock (Lade 1977). This isotropic failure criterion is expressed in terms of the first and the third stress invariants of the stress tensor as follows:

$$\eta_1 = \left( \frac{I_1^3}{I_3} - 27 \right) \left( \frac{I_1}{P_a} \right)^m \tag{1}$$

in which

$$I_1 = \sigma_1 + \sigma_2 + \sigma_3 = \sigma_z + \sigma_r + \sigma_\theta \tag{2}$$

$$I_3 = \sigma_1 \sigma_2 \sigma_3 = \sigma_z \sigma_r \sigma_\theta - \sigma_r \tau_{z\theta} \tau_{\theta z} \tag{3}$$

and  $P_a$  is atmospheric pressure expressed in the same units as the stresses. The parameters  $\eta_1$  is atmospheric pressure expressed in the same units as

LOCALIZATION EFFECTS IN TORSION SHEAR TESTS ON SAND

the stresses. The parameters  $\eta_1$  and  $m$  are constants.

Fig. 3 shows the relation between  $(I_1^3 / I_3 - 27)$  and  $(P_a / I_1)$  at failure in a full log diagram. On this diagram  $\eta_1$  is the intercept with  $(P_a / I_1) = 1$  and  $m$  is the slope of the straight line. The data from both torsion shear and cubical triaxial tests on Santa Monica Beach sand are plotted on Fig. 3. The data from conventional triaxial compression tests on Santa Monica Beach sand performed by Purabucki and Lade(1990) are also plotted on Fig. 3. The values of  $\eta_1 = 44.53$  and  $m = 0.10$  are determined from a regression analysis for the best fitting straight line on this diagram. The data of triaxial compressions in conventional triaxial, torsion shear, and cubical triaxial devices were used for the regression analysis in Fig. 3.

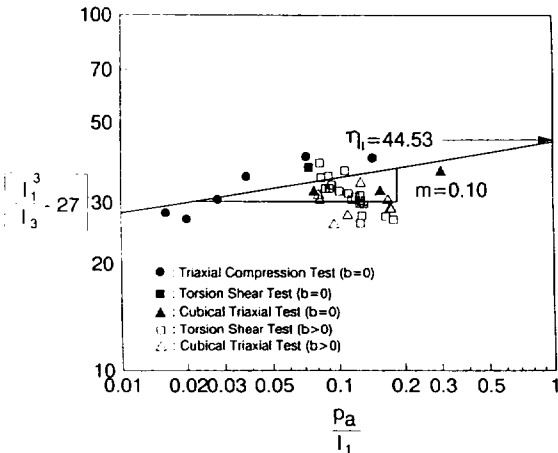


Fig. 3. Determination of material parameters  $\eta_1$  and  $m$  involved in failure criterion for Santa Monica Beach Sand.

Comparison of Failure Criterion and Torsion Shear Test Data

The strength results from the torsion shear tests are presented on a diagram of torsion shear stress,  $\tau_{\theta\theta}$ , versus vertical stress difference,  $(\sigma_z - \sigma_\theta)$ , as shown in Fig. 4. The solid curve on this diagram

represents the failure surface defined by Eq.(1). The failure surface is egg-shaped with a slightly more pointed end near the extension stress state and is symmetrical around the horizontal axis. Note that the failure surface is not an ellipse. An ellipse is obtained for the Mohr-Coulomb failure criterion.

The stresses at failure from all torsion shear tests are plotted on the torsion plane Fig. 4. The test result with compressive axial load is slightly outside the failure envelope, while the test results close to triaxial extension ( $b = 1.0$ ) were slightly inside the failure envelope. It may be seen however that the failure envelope on the torsion plane for practical purposes represents failure stresses obtained from the torsion shear tests on the tall specimens of height of 40 cm. in which the ratio of height to average diameter is 2. The experimentally obtained failure surface on the torsion plane from torsion shear tests may therefore be modeled by the isotropic failure criterion defined by Eq.(1).

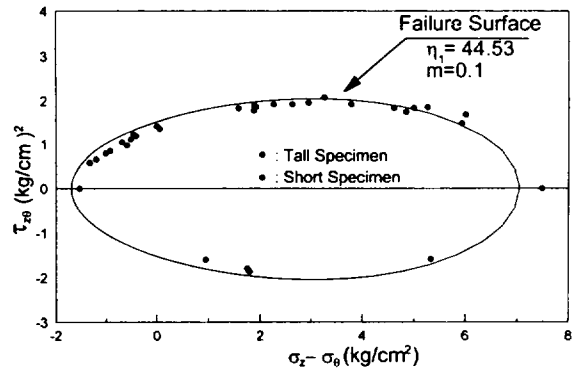


Fig. 4. Stress points at failure and failure surface shown in  $\phi$ - $b$  diagram for Santa Monica Beach Sand.

The failure envelope also can represent the failure stresses obtained from the short specimens of height of 25 cm. in which the ratio of height to average diameter is 1.25, as shown in Fig. 4. Consequently

the influence of end restraint of the tall and the short specimens on the strength of the sand are same. The ratio of height to average diameter for the short specimens coincided with almost the minimum ratio to minimize nonuniformity of stress and strain in hollow cylinder specimen presented by Lade(1981). Thus it can be confirmed that the influence of end restraint does not affect the strength when the ratio of height to average diameter of hollow cylinder specimen is higher than one.

### Effect Friction Angle

The variation of the measured effective friction angle with the value of  $b$  shown in Fig. 5. The friction angle  $\phi'$  was calculated by

$$\sin \phi' = \frac{\sigma_1 - \sigma_3}{\sigma_1 + \sigma_3} = \frac{2\sqrt{\tau_{z\theta}^2 + \frac{(\sigma_z + \sigma_\theta)^2}{4}}}{(\sigma_z + \sigma_\theta)} \quad (4)$$

The measured friction angles plotted on Fig. 5 were obtained by the torsion shear tests on the tall and the short hollow cylinder specimens. For comparison with the results of the torsion shear tests, the measured friction angles obtained by the cubical triaxial tests are also plotted on Fig. 5.

Fig. 5 shows that the variation of the friction angle to  $b$  for the short hollow cylinder specimens coincides with that for the tall specimens, whereas that for cubical specimens shows large difference from those for hollow cylindrical specimens. The variations of the friction angle to  $b$  obtained by torsion shear and cubical triaxial tests are almost same from triaxial compression to plane strain conditions. The difference of the friction angle from the two tests appears beyond plane strain condition and the largest difference between friction angle ( $\Delta\phi = 7^\circ$ ) is shown at triaxial extension condition. The measured friction angles in both tests increased initially with increasing magnitude of the

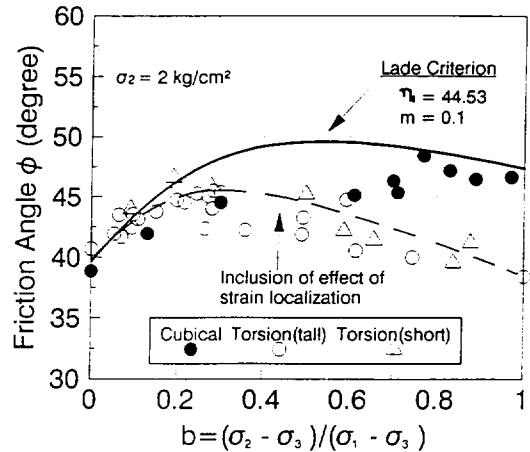


Fig. 5. Effective friction angle and failure surface shown in  $\phi$ - $b$  diagram for Santa Monica Beach Sand.

intermediate principal stress until  $b$  reached 0.3, which represents plane strain condition. Then, the friction angle in torsion shear test decreased gradually from plane strain to triaxial extension conditions, whereas the friction angle in cubical triaxial test kept essentially almost constant value until a small decrease in friction angle is appeared close to  $b=1.0$ . lubrication. Therefore, strain localization was suppressed and gross development of shear bands was impeded so that entire specimen could participate in shearing. Consequently the cubical triaxial tests produced correct strength of the sand.

On the other hand, in torsion shear tests, the geometric configuration of the boundaries was such that shear bands could develop freely without significant restraint from the soft rubber membranes that confined the specimens along the vertical sides. Thus, strain localization could develop from the beginning of shearing. The strain localization produced premature development of shear bands or necking close  $b=1.0$ . The shear bands would make the load carrying capacities of the specimen reach rapidly and reduced the strength of the sand.

The effect of strain localization on the measured



strength began at plane strain and was most significant at triaxial extension, whereas the triaxial compression test was most resistant to shear banding. Peter et al.(1988) showed a similar results from three series of tests under conditions of triaxial compression, triaxial extension and plane strain. Yamamuro and Lade(1995) also indicated that similar strain localization was repeatedly occurred in triaxial extension tests on cylindrical specimens. Therefore, the measured friction angle in torsion shear apparatus is unreliable under conditions from plane strain to triaxial extension.

The solid and the dashed lines in Fig. 5 represent the failure surfaces given by the criteria proposed by Lade(1977), and Matsuoka and Nakai(1974), respectively. Fig. 5 shows that the failure criterion by Lade appears to account for the experimental data cubical triaxial tests, whereas the failure criterion by Matsuoka and Nakai appears to account for the experimental data of the torsion shear tests. This result indicates that the strength developed under uniform strain condition can be modelled by the failure criterion proposed by Lade, whereas the strength affected by strain localization can be modelled by the failure criterion proposed by Matsuoka and Nakai.

### CONCLUSIONS

A series of drained torsion shear tests on hollow cylinder specimens of Santa Monica Beach Sand have been performed along various stress paths for the purpose of investigating the strength during rotation of principal stress axes. The strength observed in torsion shear tests was compared with the measured strength in cubical triaxial tests.

Serious strain localization was observed in the hollow cylinder specimens, whereas the cubical triaxial tests enforces uniform strain in the cubical specimens.

The measured friction angles increased initially with increasing magnitude of the intermediate principal stress until plane strain condition in both tests. Then the friction angle in torsion shear test decreased gradually due to initiating strain localization from plane strain to triaxial extension value, followed a small decrease close to triaxial extension.

Specimen geometry and boundary conditions affect measured strength, leading to different three corresponds to uniform strains.

### ACKNOWLEDGEMENTS

This study was supported by Developing Fund of Cheju National University. And these tests were performed in Johns Hopkins University. Greatful appreciation is expressed to both University for their support of this study.

### APPENDIX. REFERENCES

- Arthur, J.R.F., 1988. Cubical devices: versatility and constraints. *Advanced Triaxial Testing of Soil and Rock*, ASTM STP 977, R.T.Donaghe, R.C.Chaney and M.L.Silver eds., American Society for Testing and Materials, Philadelphia, Pa, 7-67.
- Arthur, J.R.F. and Dunstan,T., 1982. Rupture layers in granular media. *Proc., IUTAM Conf.on Deformation and Failure of Granular Materials*, Delft, 453~459.
- Arthur, J.R.F. et al., 1977. Plastic deformation and failure in granular media. *Geotechnique*, 27(1), 53~74.
- Fukushima, S. and Tatsuoka, F., 1982. Deformation and strength of sand in torsional simple shear. *Proc., IUTAM Conf. on Deformation and Failure of Granular Materials*, Delft, 371~379.
- Hong, W.P. & Lade, P.V., 1989a. Elasto-plastic

- behavior of Ko-consolidated clay in torsion shear test. *Soils and Foundations*, 29(2), 57~70.
- Hong, W.P. & Lade, P.V., 1989b. Strain increment and stress directions in torsion shear tests. *J.Geotech. Engrg. Div., ASCE*, 115(10), 1388~1401.
- Hong, W.P., Nam, J. and Lade, P.V., 1995. Effects of stress rotation in torsion shear tests on sand. Submitted to *Can. Geotech.J.*
- Lade, P.V., 1977. Elasto-plastic stress-strain theory for cohesionless soil with curved yield surfaces. *Int.J. of Solids and Structures*, Pergamon Press, Inc., New York, N.Y., 13, 1019~1035.
- Lade, P.V., 1978. Prediction of undrained behavior of sand. *J.Geotech.Engrg Div., ASCE*, 104(6), 721~735.
- Lade, P.V., 1981. Torsion shear apparatus for soil testing. *Laboratory Shear Strength of Soil*, ASTM STP.740.R.N.Yong & F.C.Townsend eds., American Society for Testing and Marerials, Philadelphia, Pa., 145~163.
- Lade, P.V., 1982a. Three-parameter failure criterion for concrete. *J. Engrg. Mech. Div. ASCE*, 108(5), 850~863.
- Lade, P.V., 1982b. Localization effects in triaxial tests on sand. *Proc., IUTAM Conf. on Deformation and Failure of Granular Materials*, Delft, 461~471.
- Lade, P.V. and Duncan, J.M., 1973. Cubical triaxial tests on cohesionless soil. *J.Soil Mech. and Found. Div., ASCE*, 99(10), 793~812.
- Lade, P.V. & Musante, H.M., 1978. Three-dimensional behavior of remolded clay. *J.Geotech. Engrg. Div., ASCE* 104(2), 193~209.
- Lade, P.V. et al., 1994. Experimental determination of constitutive behavior of soils. *Computer Methods and Advances in Geomechanics*, Siriwardane and Zaman eds., Balkema, 1, 215~222.
- Matsuoka, H. and Nakai, T., 1977. Stress-strain relation of soil based on SMP, characteristics under three different principal stress. *Proc., Specialty Session 9, 9th ICSMFE*, 153~162.
- Peter, J.F., Lade, P.V. and Bro, A., 1988. Shear band formation in triaxial and plane strain tests. *Advanced Triaxial Testing of Soil and Rock*, ASTM STP 977, R.T.Donaghe, R.C.Chaney and M.L.Silver eds., American Society for Testing and Materials, Philadelphia, Pa. 604~627.
- Purabucki, M.J. and Lade, P.V., 1990. Triaxial compression tests on Santa Monica Beach Sand. 1. Report PL-CDT-SMB-1. UCLA-ENG-91-03 Aug.
- Roscoe, K.H., Schofield, A.N., and Thurairajah, A., 1963. An evaluation of test data for selecting a yield criterion for soils. *Laboratory Shear Testing of Soils STP No.3*, American Society for Testing and Materials, Ottawa, Canada, September.
- Saada, A.S., 1988. State-of the-art: Hollow cylinder torsional devices. Their advantages and limitations. *Advanced Triaxial testing of Soil and Rock*, ASTM STP 977, R.T.Donaghe, R.C.Chaney & M.L.Silver eds., American Society for Testing and Materials, Philadelphia, Pa. 766 ~795.
- Scarpelli, G. and Wood, D.M., 1982. Experimental observations of shear band patterns in direct shear tests. *Proc., IUTAM Conf. on Deformation and Failure of Granular Materials*, Delft, 473~484.
- Talesnick, M. and Frydman, S., 1991. Simple shear of an undisturbed, soft, marine clay in NGI and torsional shear equipment. *Geotech. Test. J.* 14(2), 180~194.
- Tatsuoka, F. et al., 1990. Strength anisotropy and shear band direction in plane strain tests of sand. *Soils and Foundations*, 30(1), 35~54.
- Yamamuro, J.A. and Lade, P.V., 1995. Strain localization in extension tests on granular materials. *J. Engrg. Mech. Div., ASCE*.